Available online at www.sciencedirect.com
SCIENCE DIRECT®
International Journal of Refrigeration 27 (2004) 830–838
REVUE INTERNATIONALE DU FROID
INTERNATIONAL JOURNAL OF
refrigeration
www.elsevier.com/locate/ijrefrig

Optimization of a transcritical CO_2 heat pump cycle for simultaneous cooling and heating applications

J. Sarkar, Souvik Bhattacharyya*, M. Ram Gopal

Department of Mechanical Engineering, Indian Institute of Technology, Kharagpur 721302, India

Received 2 May 2003; received in revised form 2 February 2004; accepted 9 March 2004

Abstract

Energetic and exergetic analyses as well as optimization studies of a transcritical carbon dioxide heat pump system are presented in this article. A computer code has been developed to obtain sub-critical and super-critical thermodynamic and transport properties of carbon dioxide. Estimates for irreversibilities of individual components of the system lead to possible measures for performance improvement. The COP trends indicate that such a system is more suitable for high heating end temperatures and modest cold end temperatures. Expressions for optimum cycle parameters have been developed and these correlations offer useful guidelines for optimal system design and for selecting appropriate operating conditions.

Keywords: Optimization; Heat pump; Carbon dioxide; Thermodynamic cycle; High pressure; Modelling; Thermodynamic property

Optimisation du cycle transcritique d'une pompe à chaleur au dioxyde de carbone utilisée dans les applications de refroidissement et de chauffage simultanés

Mots-clés: Optimisation; Pompe á chaleur; Dioxyde de carbone; Cycle thermodynamic; Haute pression; Modélisation; Propriété thermodynamic

1. Introduction

Carbon dioxide based vapor compression refrigeration system was patented as far back as 1850, and this was followed by several decades of its use, mainly in marine applications. Several problems were faced with the early carbon dioxide based systems mainly due to the low critical temperature of CO_2. As a result and also with the invention of halocarbon refrigerants, carbon dioxide was slowly phased out of refrigeration and air conditioning applications. However, with the discovery of the harmful effects of the synthetic halocarbon refrigerants on environment there is a renewed interest in natural refrigerants such as carbon dioxide. Lorentzen and Pettersen [1–3] and Riffat et al. [4] through their pioneering studies have proved that the problem of low critical temperature of carbon dioxide can be effectively overcome by operating the system in

* Corresponding author. Tel.: +91-3222-282904; fax: +91-3222-255303.
E-mail address: souvik@mech.iitkgp.ernet.in (S. Bhattacharyya).

0140-7007/$ - see front matter © 2004 Elsevier Ltd and IIR. All rights reserved.
doi:10.1016/j.ijrefrig.2004.03.006

Nomenclature

c	specific heat (kJ kg^{-1} K^{-1})
COP	coefficient of performance
e	specific exergy (kJ kg^{-1})
e^*	output exergy (kJ kg^{-1})
h	specific enthalpy (kJ kg^{-1})
i	specific irreversibility (kJ kg^{-1})
$\dot{m}$	mass flow rate (kg s^{-1})
p	pressure (bar)
q	specific heat transfer (kJ kg^{-1})
R	gas constant (kJ kg^{-1} K^{-1})
s	specific entropy (kJ kg^{-1} K^{-1})
t	temperature (°C)
T	absolute temperature (K)
$\bar{T}$	average temperature
w	specific work (kJ kg^{-1})
Greek	
η	efficiency
ε	effectiveness

Subscripts

1–6	refrigerant state points
7–10	external fluid state points
comp	compressor
cooling	cooling mode
ev	evaporator
evef	evaporator external fluid
exp	expansion device
gc	gas cooler
gcef	gas cooler external fluid
heating	heating mode
ihx	internal heat exchanger
is	isentropic
max	maximum
o	ambient
opt	optimum
r	refrigerant
II	second law

transcritical region. This has led to the development of transcritical carbon dioxide cycles with the condenser replaced by a gas cooler. It is found that the use of gas cooler with heat rejection taking place over an unusually large temperature glide offers several unique possibilities such as simultaneous refrigeration and hot water heating/steam production, simpler control of capacity etc. Several theoretical and experimental studies have spurred further interest in carbon dioxide based systems in varied applications. Environment friendliness, low price, easy availability, non-flammability, non-toxicity, compatibility with various common materials, compactness due to high operating pressures, excellent transport properties are cited as some of the reasons behind the revival of carbon dioxide as a refrigerant.

Past studies indicate that carbon dioxide based systems have great potential in two sectors—in mobile air conditioning and in heat pumps for simultaneous cooling and heating. Extensive applications of carbon dioxide heat pumps were reported by Neksa [5]. Neksa et al. [6] and Yarrall et al. [7] have carried out experimental studies on a transcritical carbon dioxide heat pump prototype. Several manufacturers (mainly Japanese) have announced plans to launch heat pump water heaters based on carbon dioxide and a few more have actually launched products in the market. Although a few studies related to system performance analyses and optimization have been reported [8–10], theoretical optimization studies of such systems for simultaneous heating and cooling applications are scarce in open literature. In the present study, the first and second law analyses have been carried out on a carbon dioxide system for simultaneous cooling and heating applications. A computer code has been developed to estimate thermo-physical properties of carbon dioxide for sub-critical and super-critical regions. Based on the results, optimization of the system in terms of COP and exergetic efficiency has been carried out. Correlations are obtained for optimum discharge pressure, optimum gas cooler inlet temperature and COP at optimum conditions in terms of evaporator and gas cooler exit temperatures.

2. Thermodynamic property estimation

Span and Wagner [11] have developed a new fundamental equation in the form of Helmholtz energy based on a comprehensive study on experimental data for thermodynamic properties of carbon dioxide. Based on this seminal work a computer code 'CO2PROP' has been developed to estimate thermodynamic properties of carbon dioxide in sub-critical and super critical region. The code employs the technique based on the derivatives of Helmholtz free energy function. Efficient iterative procedures have been used to predict assorted state properties. A systematic comparison with the published property tables [11] calculated from the equation of state yields a maximum of 0.1% deviation. It may be mentioned that the present code performs much better than some of the available commercial software in the region around the critical point.

3. Process analysis and simulation

A simplified sketch of a carbon dioxide based heating and cooling system with its main components is given in

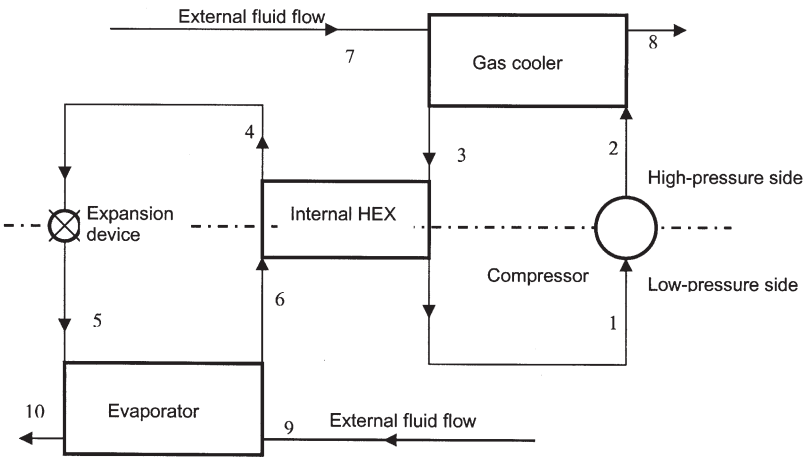

Fig. 1. Schematic diagram of a transcritical carbon dioxide system.

Fig. 1. The corresponding temperature–entropy diagram, shown in Fig. 2, is drawn employing the thermodynamic property code CO2PROP. As shown, saturated vapor at state 6 is superheated to state 1 in the internal heat exchanger and then compressed in the compressor to state 2. The supercritical carbon dioxide at state 2 is cooled in the gas cooler to state 3 by rejecting heat to the external fluid (useful heating effect). Unlike in a condenser, in the gas cooler the heat rejection takes place with a gliding temperature. Carbon dioxide at high pressure is further cooled from 3 to 4 in the internal heat exchanger. After the heat exchanger, the carbon dioxide is expanded through the expansion device to state 5, which is the inlet to the evaporator. The state of the refrigerant changes from 5 to 6 as it evaporates in the evaporator by extracting heat from the external fluid (useful cooling effect). In Fig. 2, process 1–2s is an isentropic compression process, while process 1–2 is the actual compression process. The dotted line below process 2–3 represents the external fluid being heated and dotted line above evaporating process represents the external fluid being cooled.

The entire system has been modeled based on the energy balance of individual components of the system to yield the conservations equations that follow. Steady flow energy equations based on first law of thermodynamics have been employed in each case and specific energy quantities are used. The following assumptions have been made in the analysis:

1. Heat transfer with the ambient has been neglected.
2. Single-phase heat transfer has been considered for the external fluid.
3. Compression process is adiabatic but non-isentropic.
4. Evaporation process is isobaric.

(i) Refrigerating effect of evaporator:

$$q_{ev} = h_6 - h_5 \tag{1}$$

(ii) Heating effect of gas cooler:

$$q_{gc} = h_2 - h_3 \tag{2}$$

(iii) Work input to compressor:

$$w_{comp} = h_2 - h_1 \tag{3}$$

(iv) Energy balance in the internal heat exchanger:

$$h_1 - h_6 = h_3 - h_4 \tag{4}$$

(v) Energy balance for the entire system:

$$q_{ev} + w_{comp} = q_{gc} \tag{5}$$

(vi) Energy balance for gas cooler with respect to external fluid being heated:

$$\dot{m}_{gcef} c_{p,gcef} \Delta T_{gcef} = \dot{m}_r q_{gc} \tag{6}$$

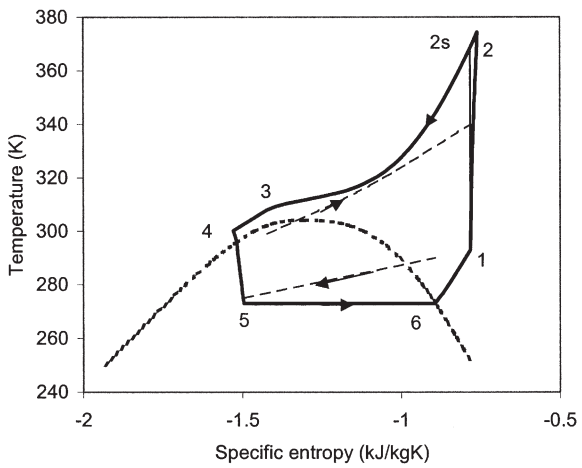

Fig. 2. Transcritical CO_2 heat pump cycle on $T-s$ plane.

where $c_{p,\mathrm{gcef}}$ is the average specific heat of external fluid being heated and $\Delta T_{p,\mathrm{gcef}}$ is its temperature rise across the gas cooler.

(vii) Energy balance in evaporator with respect to external fluid being cooled:

$$\dot{m}_{\mathrm{evef}} c_{p,\mathrm{evef}} \Delta T_{\mathrm{evef}} = \dot{m}_{\mathrm{r}} q_{\mathrm{ev}} \tag{7}$$

where $c_{p,\mathrm{evef}}$ is the average specific heat of external fluid being cooled in the evaporator and ΔT_{evef} is its temperature drop across the evaporator. COPs for the heating and cooling modes are given by:

$$\mathrm{COP}_{\mathrm{heating}} = \frac{q_{\mathrm{gc}}}{w_{\mathrm{comp}}} \quad \text{and} \quad \mathrm{COP}_{\mathrm{cooling}} = \frac{q_{\mathrm{ev}}}{w_{\mathrm{comp}}} \tag{8}$$

The effectiveness of the internal beat exchanger is given by:

$$\varepsilon = \frac{T_1 - T_6}{T_3 - T_6} \tag{9}$$

The isentropic efficiency of the compressor is given by:

$$\eta_{\mathrm{is,comp}} = \frac{h_{2\mathrm{s}} - h_1}{h_2 - h_1} \tag{10}$$

where $\eta_{\mathrm{is,comp}}$ has been calculated from the following expression [12],

$$\eta_{\mathrm{is,comp}} = 0.815 + 0.022\left(\frac{p_2}{p_1}\right) - 0.0041\left(\frac{p_2}{p_1}\right)^2 + 0.0001\left(\frac{p_2}{p_1}\right)^3 \tag{11}$$

It may be noted that the above correlation for $\eta_{\mathrm{is,comp}}$ is for a particular type of compressor, even though the analysis would exactly be the same for other types of compressor. Although real systems can have compressor isentropic efficiency dependent on the degree of superheat, this correlation is independent of superheat.

3.1. Exergy analysis

An exergy analysis has been performed for each component of the system employing the fundamental steady state equation:

Net exergy transfer from the component

= Exergy transfer due to heat transfer + Exergy transfer due to work transfer + Change in flow exergy

(i) Compressor irreversibility,

$$i_{\mathrm{comp}} = T_{\mathrm{o}}(s_2 - s_1) \tag{12}$$

(ii) Expansion process irreversibility,

$$i_{\mathrm{exp}} = T_{\mathrm{o}}(s_5 - s_4) \tag{13}$$

(iii) Internal heat exchanger irreversibility,

$$i_{\mathrm{ihx}} = T_{\mathrm{o}}[(s_1 - s_6) - (s_4 - s_3)] \tag{14}$$

(iv) Total specific exergy change of the refrigerant in the evaporator,

$$e_{\mathrm{ev}} = T_{\mathrm{o}}(s_6 - s_5) - q_{\mathrm{ev}} \tag{15}$$

Neglecting irreversibility due to pressure drop, the evaporator irreversibility is given by:

$$i_{\mathrm{ev}} = T_{\mathrm{o}}(s_6 - s_5) - q_{\mathrm{ev}} \frac{T_{\mathrm{o}}}{\bar{T}_{\mathrm{evef}}} \tag{16}$$

The exergy output of the evaporator,

$$e^*_{\mathrm{ev}} = q_{\mathrm{ev}}\left|1 - \frac{T_{\mathrm{o}}}{\bar{T}_{\mathrm{evef}}}\right| \tag{17}$$

where $\bar{T}_{\mathrm{evef}}$ is the external fluid thermodynamic average temperature,

$$\bar{T}_{\mathrm{evef}} = \frac{T_9 - T_{10}}{\ln(T_9/T_{10})}$$

(v) Total specific exergy change of the refrigerant in the gas cooler;

$$e_{\mathrm{gc}} = q_{\mathrm{gc}} - T_{\mathrm{o}}(s_2 - s_3) \tag{18}$$

Irreversibility due to heat transfer through a finite temperature difference,

$$i_{\mathrm{gc},\Delta T} = q_{\mathrm{gc}} \frac{T_{\mathrm{o}}}{\bar{T}_{\mathrm{gcef}}} - T_{\mathrm{o}}(s_2 - s_3) \tag{19}$$

where, $\bar{T}_{\mathrm{gcef}}$ is the heating fluid thermodynamic average temperature and is estimated the same way as that for the evaporator.

Irreversibility due to pressure difference:

$$i_{\mathrm{gc},\Delta P} = \left[-RT_{\mathrm{o}} \ln\left[1 - \frac{\Delta P_{\mathrm{gc}}}{P_2}\right]\right] \tag{20}$$

Hence total irreversibility in the gas cooler is given by:

$$i_{gc} = i_{gc,\Delta T} + i_{gc,\Delta P} \tag{21}$$

Thus exergy output of the gas cooler,

$$e^*_{gc} = e_{gc} - (i_{gc,\Delta T} + i_{gc,\Delta P}) \tag{22}$$

(vi) Finally combined exergy output of the system is,

$$e^*_o = e^*_{ev} + e^*_{gc} \tag{23}$$

Second law (exergy) efficiency for the system is given by the ratio of net exergy output and the work input to the compressor:

$$\eta_{II} = \frac{e^*_o}{w} \tag{24}$$

The percentage irreversibility has also been estimated to represent the contribution of each component to the total irreversibility in the system and is given by the ratio of the irreversibility of the component to the total irreversibility of the system. Based on the thermodynamic analysis presented above, a simulation code was developed. This code was integrated with the thermodynamic properties code CO2PROP to compute relevant thermodynamic parameters.

4. Optimum discharge pressure

Studies [8,9,12] show that the COP of transcritical CO_2 systems is significantly influenced by the gas cooler pressure, and interestingly non-monotonically. Hence there exists an optimum pressure where the system yields the best COP and the knowledge of the optimum operating conditions corresponding to the maximum COP is a very important factor in the design of a transcritical CO_2 cycle. The gas cooler exit temperature is dependent on external fluid inlet temperature; hence, at any discharge pressure, cooler exit temperature will be fixed for a certain fluid inlet condition. The existence of an optimum pressure for fixed cooler exit temperatures can be supported by the following argument. For cycle 1–2–3–4–5–6–1 (Fig. 3), COP for the heating mode is given by:

$$\mathrm{COP}_{\mathrm{heating}} = \frac{h_2 - h_3}{h_2 - h_1} \tag{25}$$

With increase in discharge pressure from p_2 to p'_2 for a constant cooler exit temperature of t_3, the heating coefficient of performance expression gets modified as:

$$\mathrm{COP}'_{\mathrm{heating}} = \frac{(h_2 - h_3) + \Delta h_2 + \Delta h_3}{(h_2 - h_1) + \Delta h_2} \tag{26}$$

Due to the unique behavioral pattern of carbon dioxide properties around the critical point and beyond, the slope of the isotherms is quite modest for a specific pressure range; at other pressures above and below this range, the isotherms are quite steep. As pressure increases, the quantity Δh_3 is large compared to Δh_2, as is evident from Fig. 3, and this causes an increase in the modified COP value as can be observed from Eq. (26). At a particular pressure, the COP attains a maximum value and the corresponding pressure is termed the optimum pressure for the cycle. With further increase in pressure, Δh_3 does not produce the required gain over Δh_2 and thus the COP begins to fall. The pressure range where the isotherms are fairly flat and where this beneficial gain in COP occurs varies considerably with cooler outlet temperature. Hence the gas cooler outlet temperature plays an influential role in determining the optimum operating conditions for the cycle.

5. Results and discussion

Important design and performance parameters for the carbon dioxide based heating and cooling systems are coefficient of performance, the exergetic efficiency, the various temperatures and pressures of the working fluid at hot and cold ends, and individual component irreversibility fractions. These parameters are suitably plotted to illustrate the various performance trends and optimum operating points.

The performance of the carbon dioxide system being studied for simultaneous heating and cooling applications is evaluated on the basis of heating and cooling COPs, which have been estimated for various operating conditions with a 0.5 bar step increase in compressor discharge pressure. Results are presented in terms of combined system COP, which is simply the sum of the heating and cooling mode COPs.

The variation of maximum system COP with corresponding optimum discharge pressure for various evaporator temperatures for a cooler outlet temperature of 35 °C and internal heat exchanger effectiveness of 60% is shown in Fig. 4. With an increase in evaporator temperature from − 10 to 10 °C, the system COP increases sharply recording an increase of over 75%. However, optimum pressure variation with evaporator temperature is much less significant. Although experimental results show that with increase in evaporator temperature the optimum pressure increases due to increase in cooler outlet temperature, here optimum discharge pressure exhibits a different nature due to the constraint on cooler outlet temperature. As mentioned earlier, due to divergent nature of the isotherms in the supercritical region, the COP reaches a maximum at higher values of discharge pressure for lower evaporator temperatures as shown in Fig. 4. In the present study, it is observed that the influence of internal heat exchanger effectiveness on system COP and optimum pressure is marginal. With changes in effectiveness for a cooler outlet temperature of 35 °C and an evaporator temperature of 0 °C, negligible variations occur in maximum COP and optimum compressor

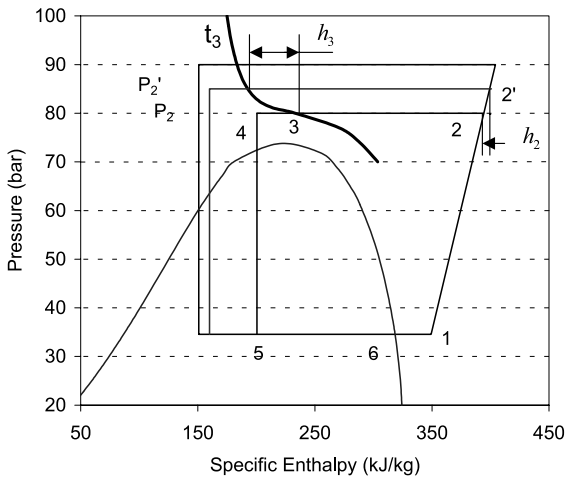

Fig. 3. $p-h$ diagram for the heat pump cycle for various gas cooler pressures.

discharge pressure. So, the performance of internal heat exchanger has a minor influence on system optimization at low and moderate gas cooler exit temperatures.

As mentioned earlier, the variation in the cooler outlet temperature has a significant impact on the optimal design conditions. The maximum system COP increases sharply with a decrease in the cooler outlet temperature as is evident from Fig. 5. For an evaporator temperature of 0 °C and an internal heat exchanger effectiveness of 60%, the system COP gets almost doubled with exit temperature falling from 50 to 30 °C and the corresponding required optimum pressure decreases from 122 to 74 bar.

5.1. Correlations for optimum conditions

The system COP depends on evaporator temperature, compressor efficiency, gas cooler outlet temperature, compressor discharge pressure and heat exchanger effectiveness:

$$\mathrm{COP} = f(t_{ev}, t_3, \eta_{is,copm}, p_2, \varepsilon) \tag{27}$$

The maximum system COP is given by, $\mathrm{COP}_{max} = f(t_{ev}, t_3, \eta_{is,copm}, \varepsilon)$ and the corresponding optimum pressure is given by, $p_{opt} = f(t_{ev}, t_3, \eta_{is,copm}, \varepsilon)$. In the present study, it is observed that for the given input temperatures the internal heat exchanger has a negligible effect on the system performance. Moreover, isentropic efficiency of the compressor is exclusively dependent on compressor design. Hence ignoring these two ($\eta_{is,comp}$ and ε) effects the optimum condition dependence reduces to its functional form expressed as:

$$\mathrm{COP}_{max} = f(t_{ev}, t_3); \quad p_{opt} = f(t_{ev}, t_3) \tag{28}$$

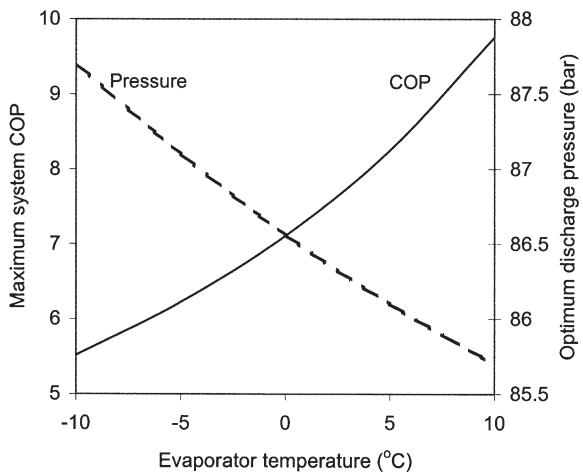

Fig. 4. Variation of maximum system COP and optimum discharge pressure with evaporator temperature.

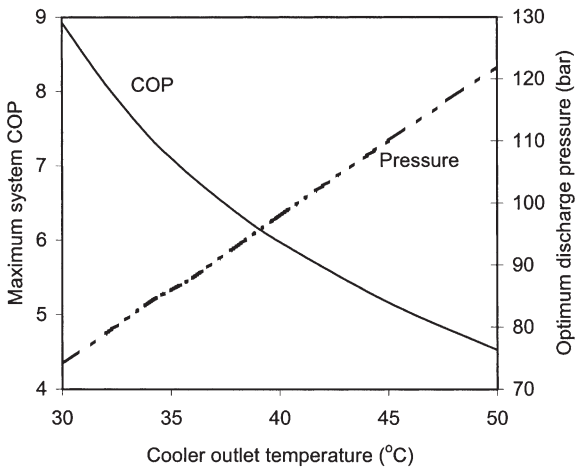

Fig. 5. Variation of maximum system COP and optimum discharge pressure with cooler outlet temperature.

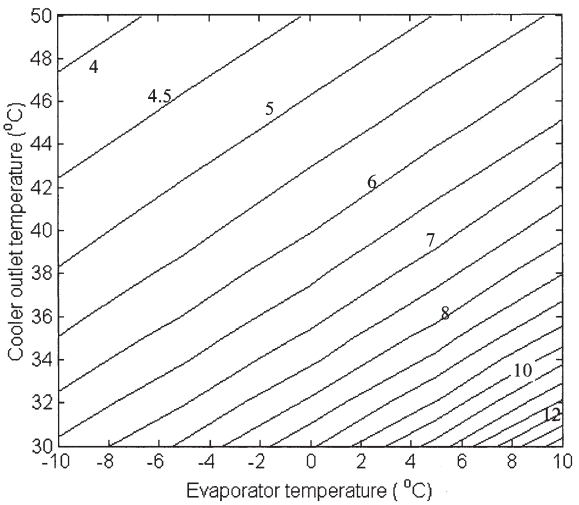

Fig. 6. Maximum system-COP contour.

Maximum system COP contours are shown in Fig. 6, where the evaporator temperature varies between −10 and 10 °C, and the gas cooler exit temperature varies from 30 to 50 °C. The maximum COP varies between 3.8 and 13.4. Iso-COP lines are fairly parallel; COP values increase from maximum cooler exit temperature and minimum evaporator temperature to minimum cooler exit temperature and maximum evaporator temperature. So to increase COP, the system has to be designed for the lowest possible cooler exit temperature and the highest possible evaporator temperature.

Optimum discharge pressure and corresponding cooler inlet temperature contours have been shown in Figs. 7 and 8, respectively, for the same range of evaporator and gas cooler exit temperatures. It may be noted that the optimum pressure varies from 73 to 123 bar and the corresponding cooler inlet temperature varies from 73 to 151 °C. Both the iso-optimum pressure lines and corresponding iso-cooler inlet temperature lines are nearly parallel and vary the least at maximum cooler exit temperature and minimum evaporator temperature as opposed to a maximum variation at minimum cooler exit temperature and maximum evaporator temperature. So to obtain useful heating at higher temperatures from the system, it has to be designed for high compressor discharge pressure, which is corresponding to maximum cooler exit temperature and minimum evaporator temperature, although the COP will be low. However, to restrict the system to lower optimum cycle pressures, it has to be designed for the minimum cooler exit temperature and the maximum evaporator temperature and gives very high COP. With increase in cooler exit temperature or decrease in evaporator temperature, the optimum discharge pressure increases. This implies that for high temperature heating or low temperature cooling the system is not profitable in term of system COP as well as cost due to high optimum discharge pressure. Keeping the smallest possible refrigerant temperature difference between evaporator and cooler outlet (yielding high COP), one can

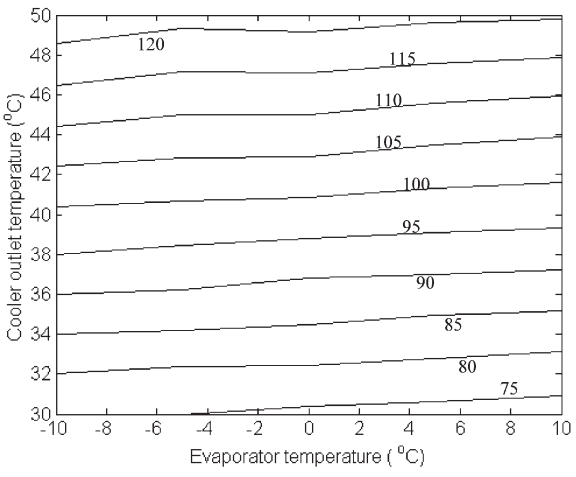

Fig. 7. Optimum discharge pressure contour (in bar).

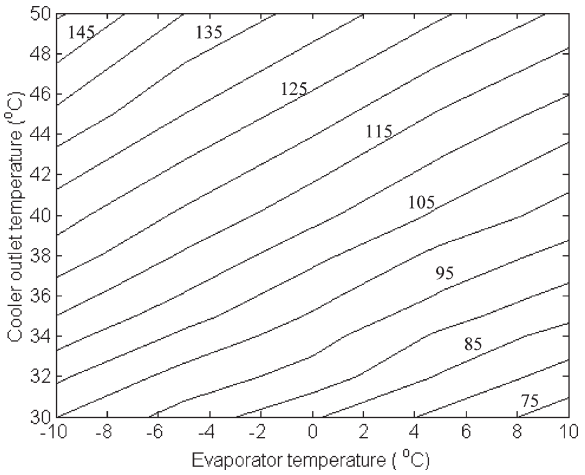

Fig. 8. Gas cooler inlet temperature (°C) at optimum discharge pressure contour.

design the system for low optimum discharge pressures (yielding lower pressure ratio) to obtain heating output at high temperature only through high superheat.

Performing a regression analysis on the data obtained from the system model explained above, the following relations have been established to predict estimates of the optimum design parameters:

$$\mathrm{COP}_{\max} = 48.2 + 0.21t_{\mathrm{ev}} + 0.05t_3(t_3 - 50) - 0.0004t_3^3,$$

$$p_{\mathrm{opt}} = 4.9 + 2.256t_3 - 0.17t_{\mathrm{ev}} + 0.002t_3^2,$$

$$t_2(at, p_{\mathrm{opt}}) = -10.65 + 3.78t_3 - 1.44t_{\mathrm{ev}} - 0.0188t_3^2 + 0.009t_{\mathrm{ev}}^2$$

These correlations are valid for evaporation temperatures (t_{ev}) ranging between −10 and 10 °C and cooler exit temperatures (t_3) ranging between 30 and 50 °C.

5.2. Exergy analysis

Second law efficiency and percentages of irreversibility for different components have been obtained for different operating conditions. For the gas cooler, mass flow rates for both refrigerant and the fluid being heated are assumed the same (1 kg/s). In the evaporator, the secondary fluid exit temperature is assumed to be 2 C above the evaporator temperature and its mass flow rate has been calculated based on unit refrigerant flow rate (1 kg/s). Inlet conditions for both secondary fluids have been taken as 10 °C lower than the cooler exit temperature. The average pressure drop in the gas cooler is taken to be 2 bar. The minimum temperature difference required at cooler outlet to avoid pinch problem in the gas cooler increases as compressor discharge pressure decreases. This behavior gets more complex in the neighborhood of the critical point and the pinch problem becomes quite significant due to the irregular constant

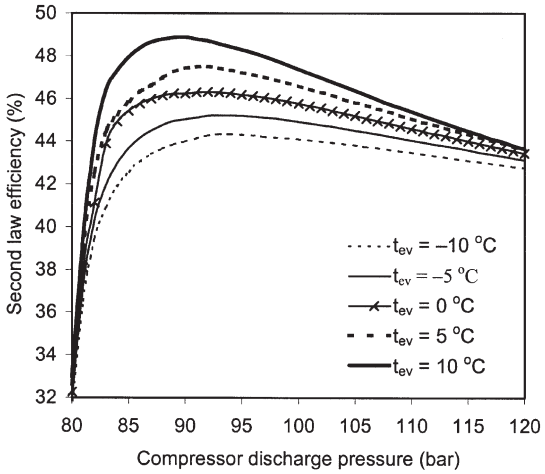

Fig. 9. Variation of second law efficiency with discharge pressure for different evaporator temperatures.

pressure line in that zone. To circumvent the pinch issue, we have taken an average temperature difference of 10 K.

Second law efficiency variations with compressor discharge pressure for various evaporator temperatures at a cooler outlet temperature of 35 °C and internal heat exchanger effectiveness 60% are presented in Fig. 9. Maximum values of second law efficiency rises from 44.3 to 48.9% with a corresponding drop in discharge pressure (from 93 to 88 bar). Calculations show that unlike its effect on COP, the heat exchanger effectiveness has some influence on the second law efficiency of the system. With increase in heat exchanger effectiveness from 0.6 to 0.9, the maximum value of second law efficiency increases by about 3%; this effect is evidently more than that on the system COP (about 1%) due to assumptions made for the secondary fluid in the heat exchanger regarding fluid temperature difference.

Second law efficiency variation with compressor discharge pressure for different gas cooler exit temperatures at

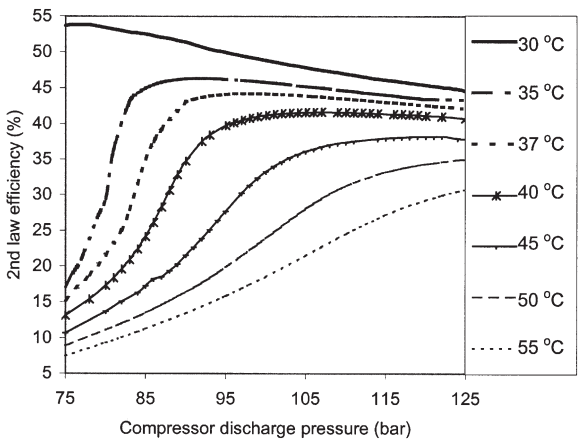

Fig. 10. Variation of second law efficiency with discharge pressure for different gas cooler exit temperatures.

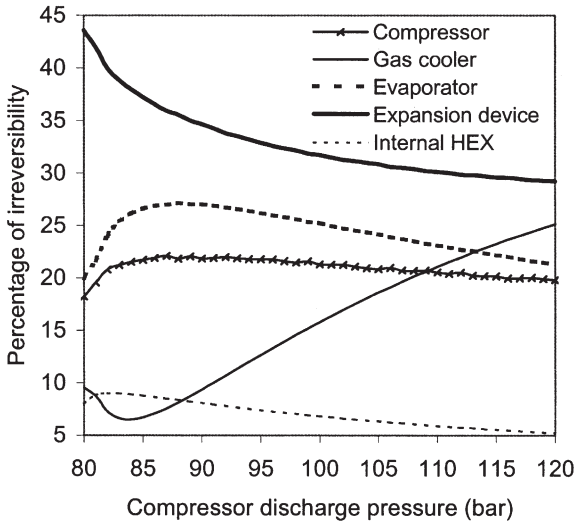

Fig. 11. Variation of percentages of irreversibility of different components with discharge pressures.

an evaporator temperature of 0 °C and internal heat exchanger effectiveness of 60% is presented in Fig. 10. With variation in gas cooler exit temperatures, maximum values of second law efficiency are found to vary widely from 53.8 to 30.8% with corresponding discharge pressure varying from 75 to 125 bar, respectively.

Fig. 11 represents the variation of percentages of total irreversibility of different components with discharge pressure at a condition specified by an evaporator temperature of 0 °C, gas cooler inlet temperature of 35 °C and internal heat exchanger effectiveness of 60%. It is observed that the effect of heat exchanger effectiveness on irreversibility is comparatively minor. It may be observed that the nature of the curves for evaporator and gas cooler are different due to different assumptions for both. Near the optimum discharge pressure, irreversibilities of compressor and evaporator are maximum but the irreversibility of gas cooler is minimum. With increase in discharge pressure, irreversibility of gas cooler increases due to increase in effective temperature difference in gas cooler heat exchanger and irreversibility of evaporator decreases due to increase in evaporation capacity. Irreversibility of compressor basically depends on isentropic efficiency of compressor, so proper design of compressor can reduce this irreversibility. To reduce the irreversibility of evaporator, evaporator heat exchanger is to be designed in such a way that the temperature difference between the fluids can be maintained as small as possible. It can be seen that the percent irreversibility of expansion valve is highest among all the components. Hence, an opportunity exists for extracting work from the expansion process by employing a turbine in place of an isenthalpic expansion valve (at least in large capacity systems).

The energy and exergy flow per unit work input (or 100%) for an optimized system at evaporator temperature of

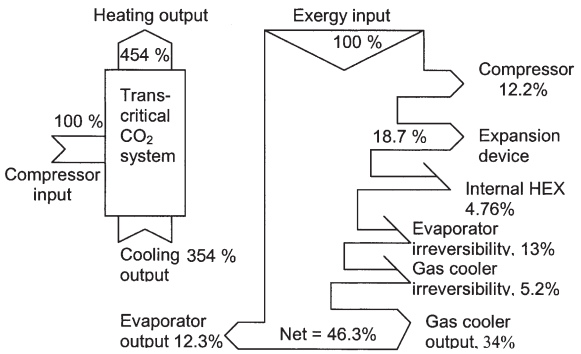

Fig. 12. Energy and exergy flow diagram.

280 K, cooler exit temperature of 310 K, internal heat exchanger effectiveness of 80%, optimum discharge pressure of 90 bar, and ambient temperature of 300 K, are shown in Fig. 12. Energy flow diagram implies that system COP is 8.08. As discussed earlier, exergy loss through expansion device is comparatively large due to large pressure difference between the two sides and also due to the distinct properties of CO_2; near the critical point the entropy as well as other properties change abruptly (as pressure drops from supercritical to supercritical). Exergy loss in the internal heat exchanger is about 4%. For the conditions stated above, irreversibility of evaporator is greater compared to that in the gas cooler because of larger average temperature difference existing across the evaporator than that in the gas cooler.

6. Conclusions

A system model and computer simulation of a transcritical carbon dioxide based simultaneous heating and cooling system with internal heat exchanger have been developed. Based on the results and optimization of the system, following conclusions can be drawn.

1. The effects of evaporator temperature and gas cooler outlet temperature are more predominant compared to internal heat exchanger effectiveness at optimized conditions for the system.
2. This system can be effectively used in process plants where heating at about 100 to 140 °C (due to the large temperature glide in the gas cooler) and simultaneous cooling/refrigeration are required. Typically, other conventional refrigerants are not able to provide outputs at these levels.
3. Analyses of the optimum condition indicate that a system meant for low or moderate temperature heating is more economical not only due to high system COP but due to lower optimum discharge pressure (low operating pressure ratio) as well. Such a system will yield good performance at lower external fluid inlet temperatures. However, it is possible to obtain high temperature heating at the expense of COP. Even though COP is lower, a system designed for such application is worthwhile because conventional refrigeration systems do not offer this high temperature heating. So there is some trade off between high COP, high outlet temperature and cost of superheating.
4. For the conditions chosen in the present study, irreversibility due to pressure drop through gas cooler is negligible compared to that due to temperature difference. So, design of all heat exchangers must involve lower temperature differences between the two fluids to yield higher second law efficiency, although that will also cause the heat exchanges to be bulkier, resulting in higher weight, cost and pressure loss.
5. Expressions for optimum cycle parameters have been developed and these correlations offer useful guidelines for optimal system design and for selecting appropriate operating conditions.

References

[1] G. Lorentzen, J. Pettersen, A new, efficient and environmentally benign system for car air conditioning, Int J Refrig 16 (1993) 4–12.
[2] G. Lorentzen, Revival of carbon dioxide as a refrigerant, Int J Refrig 17 (1994) 292–300.
[3] G. Lorentzen, The use of natural refrigerant: a complete solution to the CFC/HCFC predicament, Int J Refrig 18 (1994) 190–197.
[4] S.B. Riffat, C.F. Alfonso, A.C. Oliveira, D.A. Reay, Natural refrigerants for refrigeration and air-conditioning systems, Appl Therm Engng (1996) 33–41.
[5] P. Neksa, CO_2 heat pump systems, Int J Refrig 25 (2002) 421–427.
[6] P. Neksa, H. Rekstad, G.R. Zakeri, P.A. Schiefloe, CO_2-heat pump water heater: characteristics, system design and experimental results, Int J Refrig 21 (3) (1998) 172–179.
[7] Yarral MG, White SD, Cleland DJ, Kallu RDS, Hedley RA. Performance of a transcritical CO_2 heat pump for simultaneous refrigeration and water heating. 20th International Congress of Refrigeration, IIR/IIF, Sydney; 1999.
[8] F. Kauf, Determination of the optimum high pressure for transcritical CO_2 refrigeration cycles, Int J Therm Sci 38 (4) (1999) 325–330.
[9] S.M. Liao, T.S. Zhao, A. Jakobsen, A correlation of optimal heat rejection pressures in transcritical carbon dioxide cycles, Appl Therm Engng 20 (2000) 831–841.
[10] I.B. Vaisman, COP analysis of carbon dioxide cycle, ASHRAE Trans (2002) 252–262.
[11] R. Span, W. Wagner, A new equations of state for carbon dioxide covering the fluid region from triple point temperature to 1100 K at pressure up to 800 MPa, J Phys Chem Ref Data 25 (1996) 1509–1596.
[12] D.M. Robinson, E.A. Groll, Efficiencies of transcritical CO_2 cycles with and without an expansion turbine, Int J Refrig 21 (1998) 577–589.